

Barchans of Minqin: quantifying migration rate of a barchan

ZhenTing Wang^{1,2*}, Hui Zhao¹, KeCun Zhang¹, XiaoZong Ren²,
FaHu Chen², Tao Wang¹

1. Key Laboratory of Desert and Desertification, Cold and Arid Regions Environmental and Engineering Research Institute, Chinese Academy of Sciences, Lanzhou, Gansu 730000, China.

2. CAEP, Key Laboratory of Western China's Environmental Systems (Ministry of Education), Lanzhou University, Lanzhou, Gansu 730000, China.

*Correspondence to: Dr. ZhenTing Wang, Key Laboratory of Western China's Environmental Systems (Ministry of Education), Lanzhou University, Lanzhou, Gansu 730000, China. Tel: +86-931-8912329; E-mail: wangzht@lzu.edu.cn

Received: 23 December 2008 Accepted: 8 February 2009

ABSTRACT

The migration speed of a typical barchan on the border of Minqin oasis, Gansu Province, northwestern China, was estimated by means of two methods. One is on the basis of a simple physical model and short-term field measurements. The other comes from the combination of the barchan internal structure detected by ground-penetrating radar and optical/radiocarbon dating techniques. The upper limit of migration speed given by conventional C-14 dating is 3.42 m/yr. The optically stimulated luminescence dating indicates that the time-average migration speed of the studied barchan was 1.78 m/yr in 28 years prior to 2007. The physical estimation further suggests that the annual migration speed has increased in recent years.

Keywords: barchan; migration; sand flux

1. Introduction

The determination of migration speed is of general interest in understanding barchan dynamics. To date, three main approaches have been taken to deal with this problem. (1) Long-term field investigations including aerial and morphological surveys appear to be the most reliable method and are widely applied all over the world (Finkel, 1959; Long and Sharp, 1964; Hastenrath, 1967, 1987; Gay, 1999). Such investigations require a long time, several years at least. For example, 34 barchans on the west side of Salton Sea had been observed for 15 years (Long and Sharp, 1964). (2) The barchan migration speed can also be calculated on the base of short-term field measurements and some physical assumptions (Bagnold, 1941; Ahmedou *et al.*, 2007). It is often assumed that barchans migrate without changing their shapes. (3) Recently, Bristow *et al.*, (2005) and

Bristow and Pucillo (2006) presented a preliminary approach that combines ground penetrating radar (GPR) and optically/infrared stimulated luminescence (OSL/IRSL) dating to identify and date dune migration rates.

Minqin basin is located on the lower reaches of Shiyang River, east of Hexi Corridor in Gansu Province of northwestern China. It adjoins Tenger desert and Badain Jaran desert. The Minqin oasis, with an area of 14,400 km², is situated in the central section of the basin. At present, it is regarded as a typical region in which rapid desertification is occurring (Wang *et al.*, 2008). A detailed description of the Minqin oasis has been made (Zhang *et al.*, 2005). Previous studies of barchans in this region showed that: (1) the height of slipface is proportional to the width of horns, and the baseline can be roughly described by parts of an ellipse and a parabola (Wang *et al.*, 2007); (2) the sand flux increases with the arc length of the brink first and then decreases at both low and high wind speeds (Wang *et al.*, 2008). In this

study, we further report the estimation, by means of the latter two methods, of migration speed of a typical barchan. As far as we know, there are dozens of barchans. The highest, with a height of 9.3 m—No. A5 in our previous studies (Wang *et al.*, 2007, 2008)—was selected because suitable dating techniques for mobile and relatively younger barchans are lacking.

2. Methods

2.1. GPR survey, sampling, and dating

A 2-D GPR reflection survey was performed on the June 16, 2007, using the pulse EKKO PRO unit produced by Sensors and Software Inc. Figure 1 shows the survey lines. The 1,000 *V* transmitting antennae were employed, with central frequencies of 50 MHz and 100 MHz, separation distances of 2.00 m and 1.00 m, and sample intervals of 0.40 m and 0.20 m, respectively. The survey line topography was accurately measured using a total station (NTS-352). The GPR data process includes

dewow filtering, spherical and exponential compensation (SEC) gain, and topographic correction (Annan, 2003; Neal, 2004).

All sand samples for OSL dating were collected along the GPR survey lines. OSL sample points were selected following the principles introduced by Bristow *et al.*, (2005) and Bristow and Pucillo (2006). For sampling, a vertical hole was first drilled using specialized hand-auger equipment from Dormer Engineering Company. The sand sample was then obtained by hammering 4.0 cm diameter iron tubes into the cleaned vertical sections. The tubes were covered with a lid immediately after they had been taken from the section, and then sealed inside black plastic bags with tape to ensure the samples retained their natural water content. In the laboratory, the material at each end of the tube that may have been exposed to light was scraped away and used for water content and dose rate measurements. Coarse quartz grains of 90–150 μm diameter were prepared with the standard laboratory processes of sample preparation; luminescence measurements were completed in subdued red light.

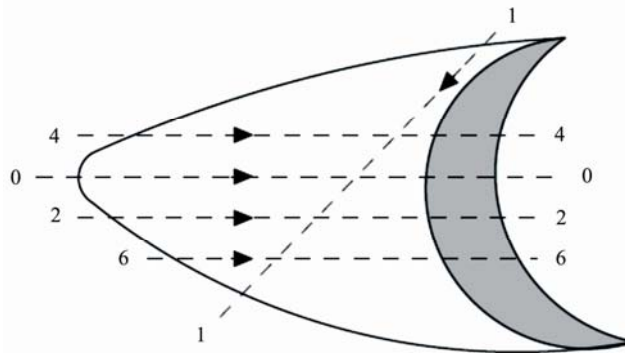


Figure 1 GPR survey lines

All raw samples were treated with 10 percent HCl and 20 percent H_2O_2 to remove carbonate and organic matter. The samples were then sieved in water to select the grain size interval 90–150 μm . This grain fraction was further separated by heavy liquid with a density between 2.62 and 2.75 g/cm^3 to obtain quartz and potassium-rich feldspar (K-feldspar) separations. After drying, the quartz grains were treated with 40 percent HF (K-feldspar grains with 10 percent HF) for 40 minutes to remove the outer layer irradiated by alpha particles. The grains were then treated with 1M HCl for 10 minutes to remove fluorides created during the HF etching. Separated sample grains were mounted on 10 mm diameter aluminum disks with silicone oil as aliquots for measurements. The OSL/IRSL measurements of samples were completed in the Luminescence Laboratory of the Cold and Arid Environment and Engineering Research Institute, CAS, using an automated RisøTL/OSL-DA-15 reader (Markey *et al.*, 1997). The OSL signal was detected through two 3.0 mm-thick Hoya U-340 filters. Laboratory

irradiation was carried out using Sr-90/Y-90 sources mounted within the readers, with dose rates 0.104 Gy/s. The U and Th concentrations and K contents were determined by means of neutron activation analysis (NAA) to estimated dose rate. The K content in K-feldspar grains was estimated as 13.5% (Zhao and Li, 2005). All concentrations were converted to alpha, beta, and gamma dose rates according to the conversion factors of Aitken (1985). The dose rate from cosmic rays was calculated on the basis of sample burial depth and the altitude of the section (Prescott and Hutton, 1994). The water content was calculated as the ratio of water weight to the dried sample weight, obtained from sample weights before and after drying in an oven.

A buried vegetated dune with the height of 0.40–0.50 m was found at the foot of the windward slope, and a C-14 sample was also collected at the depth of 0.20 m. This C-14 sample was treated following the standard program of radiocarbon dating technique at the Key Laboratory of Western China's Environmental Systems of Lanzhou University.

2.2. Physical model

In the dynamic equilibrium state, the dune migration speed v can be written as (Bagnold, 1941; Cooke and Warren, 1973)

$$v = q_c / (\rho_b H) \quad (1)$$

where q_c is the mass flux at the crest, ρ_b is the bulk density of dune, and H is the dune height.

It is obvious that the dune migration speed v critically depends on the crest mass flux q_c in equation (1). To improve the accuracy of estimation, we applied the mass flux along the brink rather than at one point. The formula for the dune migration speed can then be written as

$$v = \frac{\int_0^S q(s) ds}{\rho_b \int_0^S H(s) ds} \quad (2)$$

where s and h are the arc length and the height of the brink, respectively. The tips of two barchan horns in this study are $s=0$ m and $s=S=260$ m (Wang *et al.*, 2008).

There are various practical aeolian sand-transport equations to predict the mass flux. The equation of Lettau and Lettau described in Shao (2000) is

$$q(s) = c \sqrt{\frac{d}{D}} \frac{\rho}{D} u_*^3(s) \left(1 - \frac{u_{*t}}{u_*}\right), u \geq u_{*t} \quad (3)$$

where $c=4.2$, $D=250$ μm , d is sand grain size, g is the acceleration of gravity, ρ is air density, u_* is friction velocity, u_{*t} is the threshold friction velocity.

In equation (3), only the friction velocity $u_*(s)$ along the brink should be determined. To avoid complicated numerical computations or experiments, we can make a simple linear assumption,

$$u_*(s) = \alpha(s) u_* \quad (4)$$

where u_* is the friction velocity of incoming flow. The dimensionless parameter (α) in equation (4) reflects the wind speed-up effect which is different in weak and strong wind conditions,

$$\alpha = \alpha_1, \quad u_* \leq 4.5 \text{ m/s} \quad (5-1)$$

otherwise

$$\alpha = \alpha_2 \quad (5-2)$$

where α can be determined by our previous field observations (Wang *et al.*, 2008). Substituting equations (4) and (5) into equation (3), we obtained a simple cubic equation about α . The change of α with the arc length s is shown in Figure 2.

Detailed wind-velocity data in the period between 2000 and 2005 were provided by the Minqin meteorological station. The average wind speed over 10 minutes was used to represent the corresponding one-hour wind speed while estimating the barchan migration speed. For the flat terrain we studied, such treatment of wind velocity is reasonable and practical.

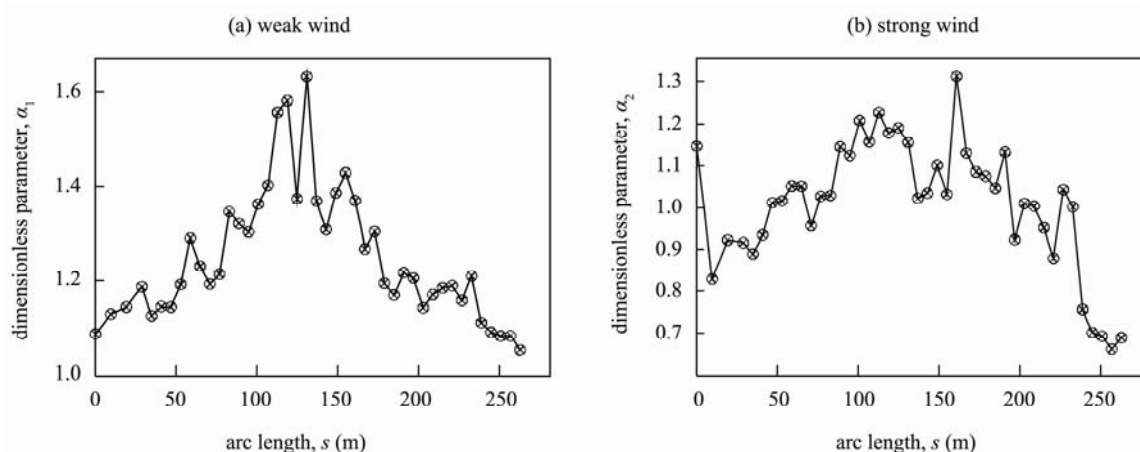


Figure 2 Change of α with s

3. Results and discussions

Figure 3, in which the depth was calculated by the typical speed (of 0.15 m/ns) of electromagnetic field for dry sand, shows the GPR profile of the barchan along its symmetrical axis. The internal structure of the barchan is very simple and in accord with Bagnold's model (Bagnold, 1941;

Pye and Tsoar, 1990). As shown in Figure 3a, the grain-flow laminae constitute the dominant primary structure. The 100 MHz antennae detected more detailed stratifications, some of which reflect the influence of reverse wind, as seen in Figure 3b. The clay layer and the ancient dune under this modern barchan should be helpful for the study of paleo-environmental changes in this region.

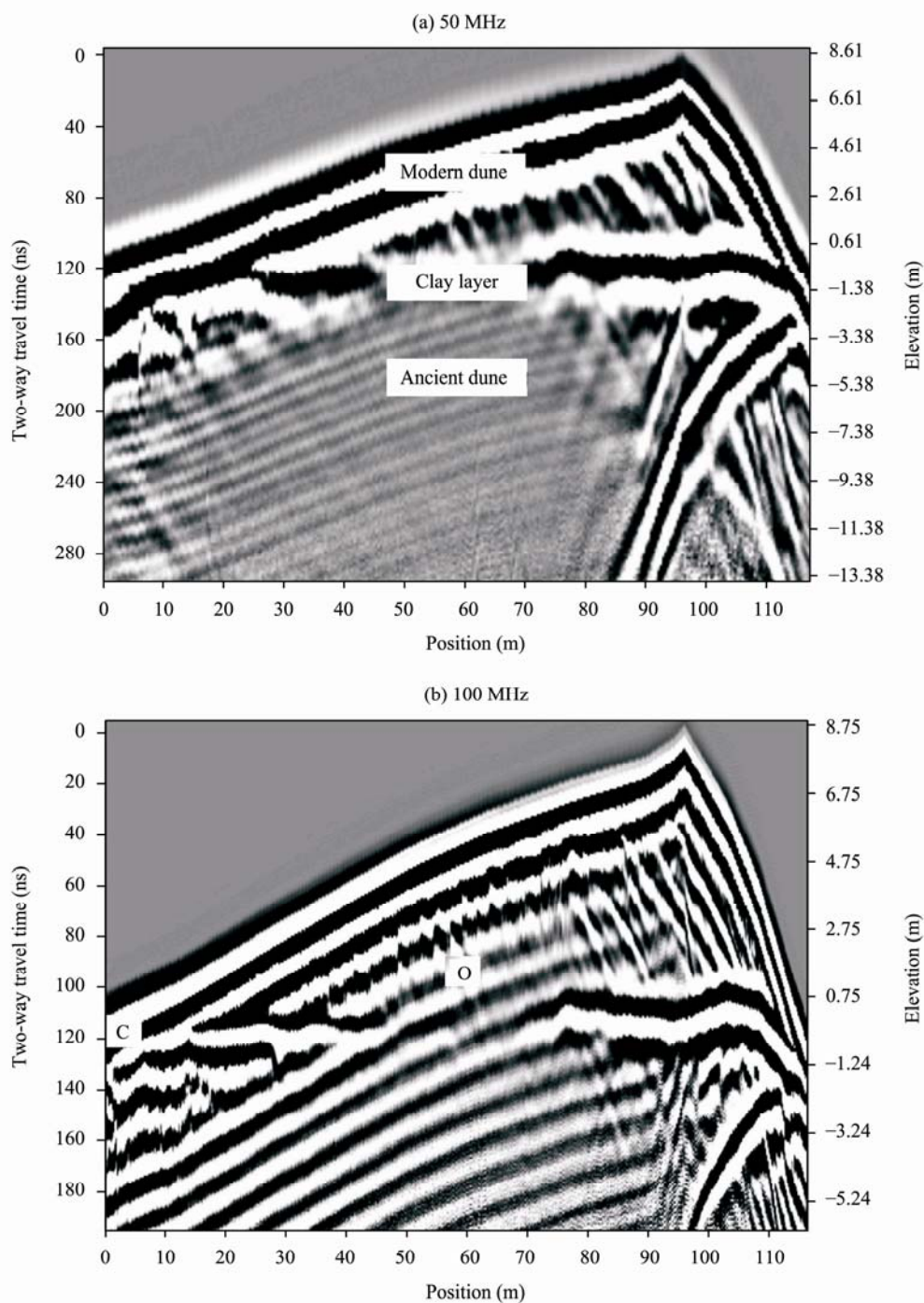


Figure 3 GPR profile of 0–0 section: "O" OSL sample, "C" C-14 sample

The percentage of modern carbon in the wood sample collected from the buried small dune is 140.43. By comparing the sample with Delta C-14, the proxy for atmospheric CO₂ in the northern hemisphere temperate region, *i.e.*, the comparison of "C" to "O" in Figure 3b (Park *et al.*, 2002), it was revealed that the C-14 age is calculated to be 1963 AD or 1975 AD. The plants associated with the small nabkha must be dead after being buried by the mobile barchan. Thus,

the upper limit of the time-average migration speed of the barchan, derived from the C-14 age, is 3.42 m/yr.

In luminescence dating methods, the event being dated is the last exposure of the grains to daylight (Duller, 2004). During the OSL measurements, the quartz grains have signals so dim that they could hardly be distinguished from background values. It was impossible to get equivalent dose (*De*) from quartz separations. The K-feldspar separations

were used for dating because the K-feldspar has higher sensitivity to dose and has distinct advantages over quartz for dating samples younger than 100 years (Li *et al.*, 2007). However, it seems that most samples have not enough IRSL signals for dating (Figure 4a). Only sample L2007-51 had weak signals that could be distinguished from background

values (Figure 4b). It has an OSL age of 28 ± 17 years. This means that the time-average migration speed of the studied barchan is 1.78 m/yr in the 28 years before 2007. It should be pointed out that, with the improvement of dating techniques, the estimation of dune migration rate would be more accurate.

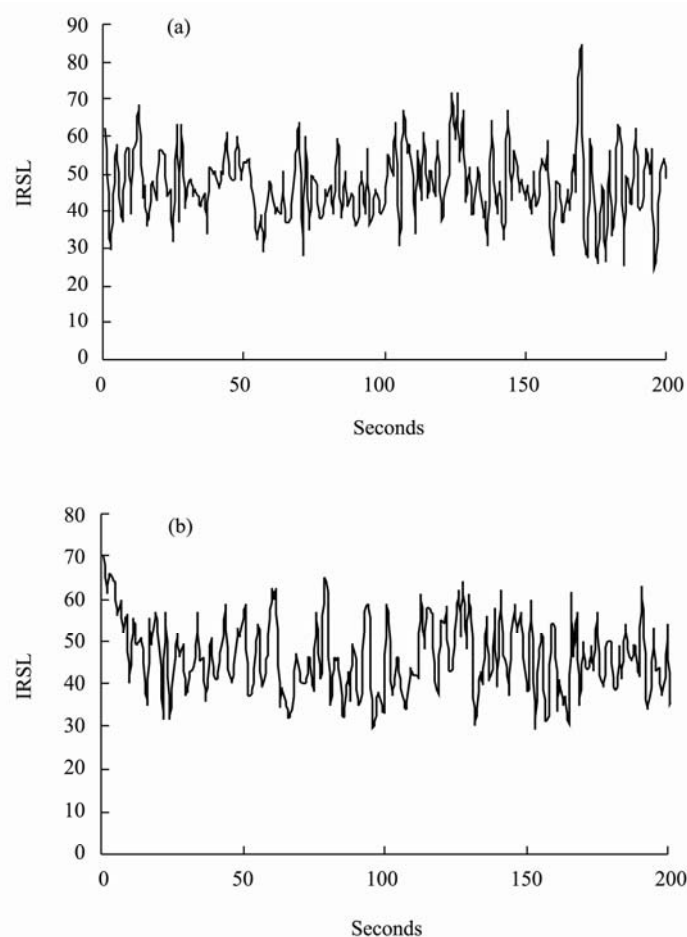


Figure 4 The IRSL signal of samples (a) the natural signal from most of the samples. (b) the natural signal from sample L2007-51, it has weak signal above the background.

Table 1 The migration of the barchan based on the physical model and short-term wind data, scale in cm

Month	2000	2001	2002	2003	2004	2005
Jan.	0.2	1.3	3.2	11.5	3.6	0.5
Feb.	0.6	0.5	15.4	3.6	62.4	18.0
Mar.	1.0	1.7	49.7	16.0	54.2	0.2
Apr.	2.8	1.8	41.7	58.3	14.3	30.4
May	***	0.3	10.1	8.8	26.0	33.9
Jun.	0.0	0.6	7.3	7.2	5.8	5.8
Jul.	0.3	0.9	0.1	4.5	3.6	5.1
Aug.	0.2	***	-4.8	0.6	-3.6	1.1
Sep.	0.2	0.0	7.6	10.4	3.7	0.7
Oct.	0.1	0.5	18.6	15.2	7.5	1.0
Nov.	0.1	0.0	18.5	12.0	1.2	17.3
Dec.	0.0	0.9	4.0	4.1	14.5	10.3
Total	6.9	9.0	171.4	152.2	193.2	124.3

Table 1 lists the migration of the barchan based on the physical model and short-term wind data. Note that the field observed migration distance of the barchan is in the range of 1.0–1.5 m from March 2006 to March 2007, this estimation is acceptable. Compared with the period of 2002 to 2005, the migration during 2000 to 2001 can be ignored. So, it appears that the annual migration speed of the studied barchan has increased in recent years.

4. Conclusions

The work presented here suggests the following:

(1) Both methods, *i.e.*, dating and physical models, are valid for estimating barchan migration in this study, although dating techniques need to be improved.

(2) The upper limit of the time-average migration speed of the barchan, given by the conventional C-14 dating, is 3.42 m/yr.

(3) The time-average migration speed of the barchan, based on OSL dating, is 1.78 m/yr in the 28 years prior to 2007.

(4) The annual migration speeds of mobile dunes in the Minqin region have increased in recent years.

Acknowledgments:

Thanks are given to GuoQiang Li and ShiChen Tao for their help in the field investigation. Thanks as well to ZongLi Wang for his assistance in the radiocarbon dating analysis. This research was supported by 973 project No. 2000048700, NSFC projects No. 40601053 and 40872108, and Ministry of Science and Technology of China project No. 2006FY110800.

REFERENCES

- Ahmedou DO, Mahfoudh AO, Dupont P, Moctar AOE, Valance A, Rasmussen, KR, 2007. Barchan dune mobility in Mauritania related to dune and interdune sand fluxes. *Journal of Geophysical Research*, 112, F02016.
- Aitken MJ, 1985. *Thermoluminescence Dating*. Academic Press, London.
- Annan AP, 2003. *Ground Penetrating Radar Principles, Procedures and Applications*, 157–175. Sensors & Software Inc.
- Bagnold RA, 1941. *The Physics of Blown Sand and Desert Dunes*. Methuen, New York.
- Bristow CS, Lancaster N, Duller GA, 2005. Combining ground penetrating radar surveys and optical dating to determine dune migration in Namibia. *Journal of the Geological Society of London*, 162: 315–321.
- Bristow CS, Pucillo K, 2006. Quantifying rates of coastal progradation from sediment volume using GPR and OSL: the Holocene fill of Guichen Bay, southeast South Australia. *Sedimentology*, 53: 769–788.
- Cooke RU, Warren A, 1973. *Geomorphology in Deserts*. UCL Press, London.
- Duller GAT, 2004. Luminescence dating of Quaternary sediments: recent advances. *Journal of Quaternary Science*, 19: 183–192.
- Finkel HJ, 1959. The barchans of southern Peru. *Journal of Geology*, 67: 614–647.
- Gay Jr SP, 1999. Observations regarding the movement of barchan sand dunes in the Nazca to Tanaca area of southern Peru. *Geomorphology*, 27: 279–293.
- Hastenrath RL, 1967. The barchans of the Arequipa region, southern Peru. *Zeitschrift für Geomorphologie*, N.F. 11: 300–331.
- Hastenrath RL, 1987. The barchan dunes of southern Peru revisited. *Zeitschrift für Geomorphologie*, N.F. 31: 167–178.
- Li, SH, Chen, YY, Li B, Sun J, Yang, LR, 2007. OSL dating of sediments from deserts in northern China. *Quaternary Geochronology*, 2: 23–28.
- Long JT, Sharp RP, 1964. Barchan-dune movement in the Imperial Valley, California. *Geological Society of America Bulletin*, 75: 149–156.
- Markey BG, Botter-Jensen L, Duller GAT, 1997. A new flexible system for measuring thermally and optically stimulated luminescence. *Radiation Measurements*, 27: 83–90.
- Neal A, 2004. Ground-penetrating radar and its use in sedimentology: principles, problems and progress. *Earth-Science Reviews*, 66: 261–330.
- Park JH, Kim JC, Cheoun MK, Kim IC, Youn M, Liu YH, Kim ES, 2002. 14 C level at Mt Chiak and Mt Kyeryong in Korea. *Radiocarbon*, 44: 559–566.
- Prescott JR, Hutton JT, 1994. Cosmic ray contributions to dose rates for luminescence and ESR dating: large depths and long-term time variations. *Radiation Measurements*, 23: 497–500.
- Pye K, Tsoar H, 1990. *Aeolian Sand and Sand Dunes*. Unwin Hyman Ltd, London.
- Shao YP, 2000. *Physics and Modelling of Wind Erosion*. Kluwer Academic, Dordrecht.
- Wang XM, Chen FH, Hasi E, Li JC, 2008. Desertification in China: An assessment. *Earth Science Reviews*, 88: 188–206.
- Wang ZT, Tao SC, Xie YW, Dong GH, 2007. Barchans of Minqin: morphology. *Geomorphology*, 89: 405–411.
- Wang ZT, Zhang JW, Zhang QH, Qiang MR, Chen FH, Ling YQ, 2008. Barchans of Minqin: sediment transport. *Geomorphology*, 96: 233–238.
- Zhang K, Qu J, Zu R, Fang H, 2005. Temporal variations of sandstorms in Minqin oasis during 1954–2000. *Environmental Geology*, 49: 332–338.
- Zhao H, Li SH, 2005. Internal dose rate to K-feldspar grains from radioactive elements other than potassium. *Radiation Measurements*, 40: 84–93.